Elucidating the pathogenesis underlying bicuspid aortic valve disease using new disease models

Pol, V. van de

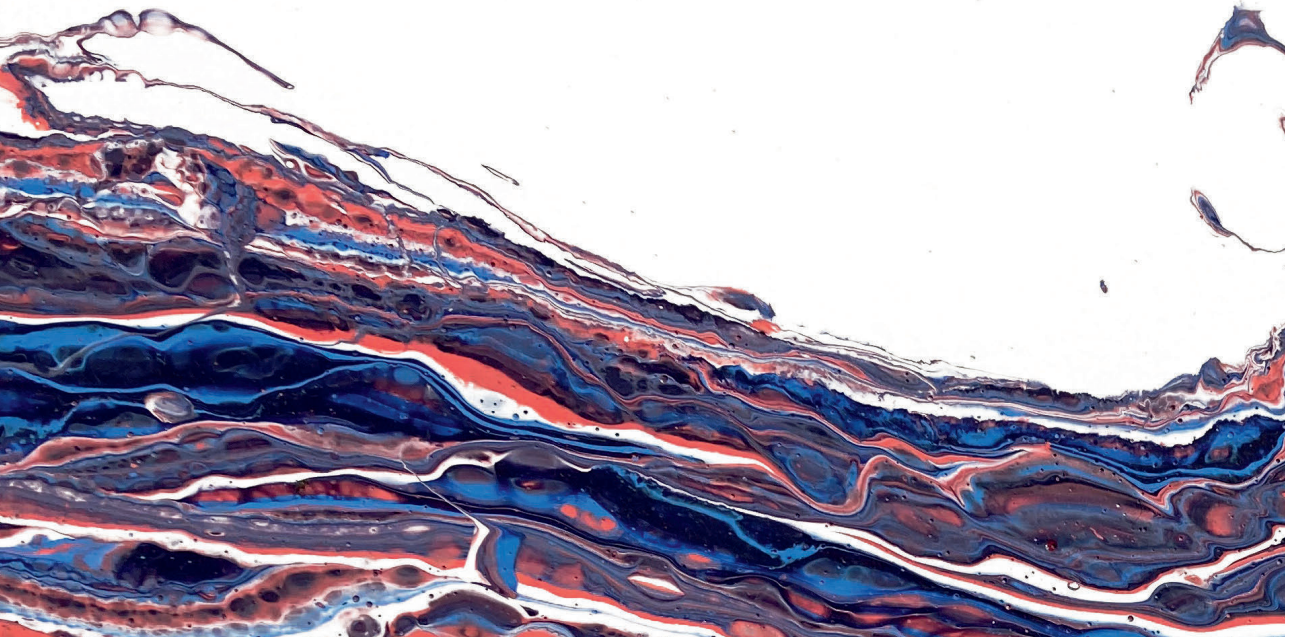

Chapter 3

Higher expression of inflammatory and EndoMT markers in endothelial cells in the inner aortic curve of bicuspid aortic valve patients

Vera van de Pol[1], Zuzana Miranovova[1], Nimrat Grewal[2], Adri C. Gittenberger-de Groot[3,4], Evaldas Girdauskas[5], Marie-José Goumans[1], Marco C. DeRuiter[3]

[1] Department of Cell and Chemical Biology, Leiden University Medical Center, Leiden, The Netherlands
[2] Department of Cardiothoracic Surgery, Leiden University Medical Center, Leiden, The Netherlands
[3] Department of Anatomy and Embryology, Leiden University Medical Center, Leiden, The Netherlands
[4] Department of Cardiology, Leiden University Medical Center, Leiden, The Netherlands
[5] Department of Cardiac Surgery, Heart Center, Zentralklinik Bad Berka, Germany

Study in progress

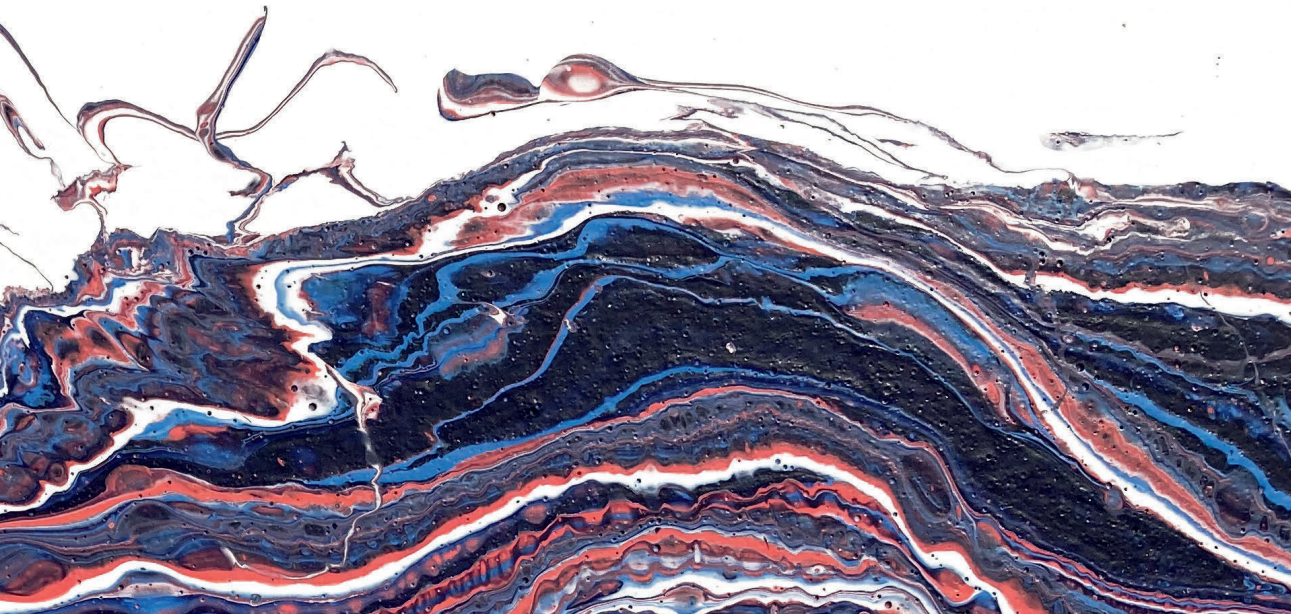

Abstract

Bicuspid aortic valve (BAV), in which the aortic valve consists of two leaflets instead of the usual three, is the most common congenital heart defect. The shape of a BAV causes a different blood flow within the ascending aorta compared to a tricuspid aortic valve, exposing one side of the aortic wall to an increased blood flow velocity ("jet side") and the opposing side to an oscillatory flow ("non-jet side"). Different types of flow can affect the endothelium and thereby vessel wall homeostasis, but it is not known whether the altered flow in BAV affects endothelial cell (EC) phenotype in the aorta. Therefore, the aim of this study was to investigate if these flow differences in BAV patients activate the endothelium.

Aortic samples from the two opposing sides of the aorta were collected during surgery and the intima and inner media were histologically examined. The structural organization was assessed measuring the amount of elastin and the intimal thickness while the activation was studied with a staining for von Willebrand Factor (vWF). In addition, markers of endothelial-to-mesenchymal-transition (EndoMT) (SNAI1), proliferation (KI67) and inflammation (p50) were investigated in $PECAM^+$ ECs.

Whereas there were no observable differences in $elastin^+$ surface area in the intima and inner media between jet and non-jet side, we observed a significantly larger area of tissue containing deposited vWF at the jet side of the aorta of BAV patients compared to the non-jet side. In contrast, the $PECAM^+$ ECs showed a trend towards higher expression of SNAI1, KI67 and p50 at the non-jet side compared to the jet side, indicating increased endothelial activation at the non-jet side. In conclusion, the endothelium at the jet site of the BAV aorta shows a different protein expression of activation markers compared to the non-jet side of the aorta.

Introduction

Bicuspid aortic valve (BAV), a congenital defect in which the aortic valve consists of two leaflets instead of the usual three, is the most common congenital heart defect occurring in approximately 1-2% of the population. Although a BAV can function normally, BAV patients have an increased prevalence of thoracic aortic aneurysm and rupture, as well as aortic valve regurgitation and stenosis [1].

The thoracic aorta in BAV patients dilates because of a loss of structural integrity in the medial layer of the aorta called medial degeneration. Medial degeneration is the process during which elastic lamellae become fragmented (by elastases produced by smooth muscle cells (SMCs) and inflammatory cells or decreased elastin turnover) and SMCs undergo phenotypic switching from a contractile to an activated synthetic phenotype [2-5]. Despite extensive research, it is not well understood how medial degeneration is initiated.

Using 4D MRI it is shown that the disturbed/malformed opening of the BAV alters the blood flow causing a focussed 'jet' that hits the aortic wall, thereby locally increasing wall shear stress [6,7]. Conversely, the opposing side of the aorta is subjected to turbulent flow. The flow-hypothesis is based on these observations and states that the aortic dilation in BAV patients is caused by the altered flow. Supporting this hypothesis are, amongst others, results showing that local differences in flow patterns relate to the underlying histopathological logical features [8-12].

Different types of flow are known to highly affect endothelial function, which in turn affects vessel wall homeostasis. Laminar flow maintains a quiescent EC state, promoting vessel wall homeostasis, whereas turbulent flow can activate the endothelium, stimulating vascular remodeling. Activated ECs are part of a normal vascular healing response but also of many different cardiovascular diseases. Activated ECs are characterized by an increased proliferation rate, expression of inflammatory markers and secretion of Von Willebrand factor [13-15]. To date, little research has been performed to elucidate the role of endothelial cells in the pathogenesis of BAV related aortic aneurysm.

To study the effect of flow differences on the aortic structure, we made use of a collection of aortic samples from the jet and non-jet side of the aorta from BAV patients. A previous study using these specimens demonstrated a dispersion of the elastic lamellae and decreased α-smooth muscle actin (αSMA) expression in the media located at the jet side of the aorta [12]. To relate the vessel wall structure to endothelial activation, we investigated elastin morphology in the vessel wall located directly underneath the endothelium. Moreover, we focused on endothelial activation caused by flow differences within the aortas of BAV patients by measuring vWF deposition and the expression of the inflammatory

marker p50, the proliferation marker KI-67 and the EndoMT marker SNAI1 in ECs at the jet and non-jet side of the BAV aortic wall.

Results

More vWF deposition at the jet side of the BAV aorta

To study the intima/inner media organization and vWF secretion, samples from the jet and non-jet side of the aorta of 17 BAV patients were analysed (Table 1). The gender distribution and prevalence of type 1 and type 2 BAV of these patients reflect the known population distributions [16,17].

Table 1. Patient information

	BAV patients (n=17)
Age at time of operation, years (SD)	55.5 (9.8)
Female gender	23.5%
Aortic diameter, mm (SD)	44.6 (7.8)
Type I fusion	82.4%
Type II fusion	17.6%

Since activated ECs can secrete vWF, not only in the blood but also into the tissue, the expression of vWF is not limited to the ECs but can also be identified in the subendothelial extracellular matrix. Before quantifying the VWF expression we noticed that the areas positive for vWF show large variation between patients as well as within the aortic wall of one patient. Because of spatial differences within the tissue samples, both the average (A) percentage of vWF positive area per aortic wall sample and the area with the lowest (L) and highest (H) percentage positive for vWF were used for the analysis. All three approaches to analyse the expression showed significantly higher areas positive for vWF at the jet side compared to the non-jet side (jet: M=16.6% (A) | 11.7% (L)| 22.7% (H), SEM=2.7% (A)| 2.2%(L)| 3.7% (H), non-jet: M=9.5% (A)| 6.1% (L)| 12.6% (H), SEM=1.5% (A)| 1.3% (L)| 2.2% (H), p=0.035 (A)| 0.013 (L)| 0.046 (H)) (Figure 1A,B and Supplemental figure 1A,B).

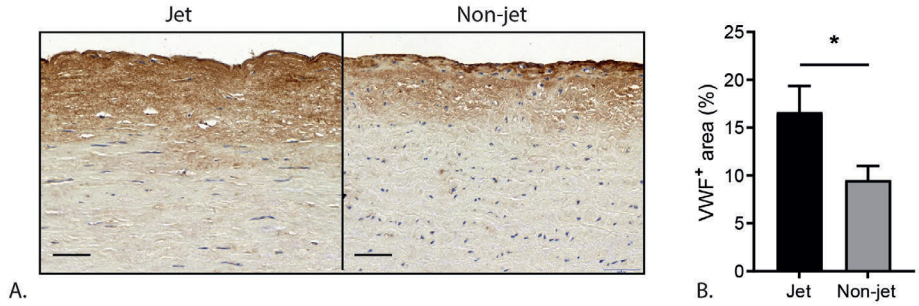

Figure 1. Intimal and inner medial expression of vWF in jet and non-jet aortic wall samples of BAV patients. A. Representative pictures of the vWF staining in jet and non-jet aortic wall samples from BAV patients. B. Quantification of the average vWF$^+$ area in jet and non-jet aortic wall samples as % of the surface area of the inner media (500 μm). Bar indicates 50 μm. *p>0.05.

Amount of elastin fibers and intimal thickness do not differ between jet and non-jet side

Taking a closer look at the elastin morphology, we observed thick and thin elastin fibers (Figure 2A). Resorcin-Fuchsin (RF) staining was used to visualize the elastic fibers. To determine whether differences in the amount of elastin co-occurred with differences in flow, the RF$^+$ surface area was quantified. However, there were no differences in the RF$^+$ surface area between jet and non-jet side (Figure 2B). To study intimal growth the thickness of the intimal layer up to the first elastic lamella was measured. No differences between jet and non-jet intimal thickness was observed (Figure 2C).

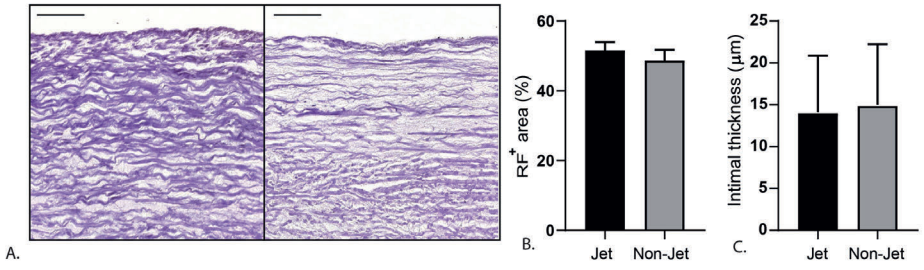

Figure 2. Intimal and inner media analysis on jet and non-jet side of BAV patient aortas. A. Representative pictures of the RF staining showing thick (left) and thin (right) elastic lamellae. B. Graph showing data of RF quantification. C. Thickness of layer up to the first elastic lamella in jet and non-jet side of BAV patients. Bar indicates 50 μm. *p>0.05.

Trends towards higher activation at the non-jet side

Because immunohistochemistry for vWF can indicate both secreted vWF and vWF present in ECs, vWF expression in tissue is a limited indicator for EC activation. Therefore, we used patient specimens in which PECAM$^+$ ECs could be detected to further study endothelial activation. Due to the fragile nature of the endothelium, only limited samples still contained PECAM$^+$ ECs (n=6, Table 2). No significant differences were observed in the patient characteristics between the total sample population and the selected samples with ECs (data not shown).

Table 2. Patient information selection for PECAM$^+$ ECs

	BAV patients (n=6)
Age at time of operation*, years (SD)	55.8 (12.8)
Female gender*,	16.7%
Aortic diameter*, mm (SD)	52.5 (4.8)
Type I fusion	83%
Type II fusion	17%

To standardize the area in which the ECs were quantified, the location with the least structured organization and αSMA and elastic lamellae in the inner media was selected for analysis. In order to assess the state of inflammation in the aortic endothelium, a co-staining for both PECAM and p50, a subunit of NFκB, was performed (Figure 3A,B). Although an increase of p50$^+$ PECAM$^+$ ECs in the non-jet side was observed, this difference did not reach significance. Signaling pathways for proliferation (ki67) and EndoMT (SNAI1) showed the same trend towards higher expression in PECAM$^+$ ECs of the non-jet side when compared to the jet side of BAV aorta (Figure 3C-F).

Because KLF2 and KLF4 have been shown to be important flow-responsive transcription factors, we determined their expression [18]. Although KLF2 and KLF4 positive ECs were present in multiple samples, at the location with the least structured organization and αSMA and elastic lamellae in the inner media no KLF2/KLF4 expression was observed (Supplemental figure 2A/B and data not shown).

Discussion

The usual laminar flow in the aorta is altered in BAV patients due to the different leaflet morphology. Instead, the aortic wall is exposed to a high velocity jet flow on one side and an oscillatory flow on the opposing side in BAV patients. This study focussed on the effect of both the high velocity jet flow and oscillatory

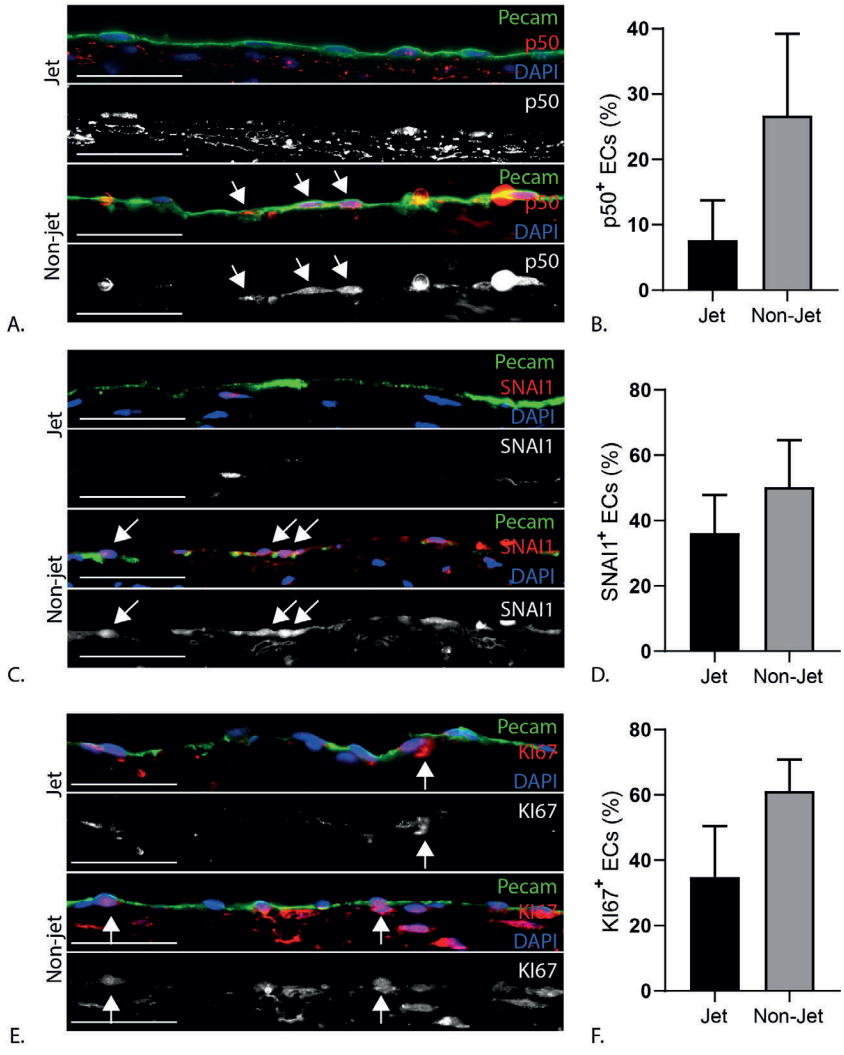

Figure 3. Endothelial activation in the jet and non-jet side of BAV aorta. A,C,E. Representative images showing Pecam staining combined with p50 (A), SNAI1 (B) and KI67 (E) in BAV tissue from jet and non-jet side. B,D,F. Quantifications of the p50 (B), SNAI1 (E) and KI67 (F) positive ECs on jet vs non-jet side. Bar indicates 50 μm. Arrows indicate double positive cells.

flow on endothelial activation in the aorta of BAV patients. Samples from aortas of BAV patients showed a higher amount of vWF expression in the intima and inner media at the jet side of the aorta compared to the non-jet side. In contrast, a trend towards increased expression of inflammatory, EndoMT and proliferation pathways in was observed in PECAM$^+$ECs exposed to oscillatory flow at the non-

jet side. The flow responsive proteins KLF2 and KLF4 were only sporadically expressed in these dilated aortic walls.

ECs are able to regulate vWF secretion and secrete vWF both under basal conditions and in an activated state [19,20]. Flow and wall shear stress are important determinants in vWF biochemistry and secretion. Since an increased wall shear stress has been shown to stimulate vWF function and secretion, our results could indicate a higher activation of the endothelium at the jet side compared to the non-jet side [21]. Most knowledge on vWF concerns vWF secreted in the blood while only little is known on the function and biochemistry of vWF deposited within the tissue. vWF can be secreted when endothelial cells are activated, but the diverse conditions in which vWF is secreted are not fully known. In addition, it is unclear how long secreted vWF remains detectable in tissue. Therefore, the cause of vWF deposition is difficult to conclude from a staining, limiting direct conclusions on the pathological endothelial activation based solely on vWF secretion in the aortic tissue. Interestingly, it has been shown that vWF secretion can cause an increase of EndoMT in osteosarcoma derived ECs *in vitro [22]*. However, in our data no relation between vWF^+ area and $SNAI1^+$ ECs was observed. This may be explained by a separation of these different processes by time or could be caused by the limited sample numbers.

In contrast to previous results obtained by studying the media of these samples, we did not find differences in elastin surface area in the intima and inner media between the jet and non-jet side [23]. A previous study by Guzzardi et al. reported that increased wall shear stress correlates with decreased elastin content in BAV aorta [24]. However, our results are obtained by focussing specifically on the inner 250 μm of the aorta (inner media/intima) whereas Guzzardi et al. used the elastin content of the entire vessel wall. These differences could indicate that the degenerative processes locate mainly in the middle of the vessel wall.

To study the endothelial protein expression in relation to laminar jet and oscillatory flow, ECs were labelled with an antibody against $PECAM^+$. Only limited samples were available in which both the jet and non-jet side of the aorta had enough $PECAM^+$ ECs to analyse. The characteristics of the patients of which the samples qualified do not significantly differ from the total population. Therefore, the lack of ECs in the majority of the samples is likely due to the fragile nature of the intima and the damage it sustains during surgical removal of the tissue.

Endothelial were shown to upregulate gene expression of pathways such as proliferation and organization of the cytoskeleton upon altered flow [25]. Prolonged exposure to a new flow speed or direction will cause adaptation of the ECs and reduce the activation of these pathways back to baseline [26]. Constantly changing oscillatory flow however, causes a chronically activated and patho-

logical phenotype [27]. The results in this study support the hypothesis that this activated EC state is caused by the oscillatory flow conditions in the BAV aorta at the non-jet side, but not by the constant laminar jet flow at the opposing side.

The BAV samples show a trend towards a higher endothelial p50 expression at the non-jet side compared to the jet side. This result is in line with previous studies on inflammation and oscillatory flow, showing an increased inflammatory response in ECs when there are exposed to oscillatory flow [13,28,29]. The role of inflammation in medial degeneration of BAV the aorta remains disputed [30,31]. However, no study thus far has focussed on the endothelial expression of inflammatory markers in the aorta. Previously we have shown that, after exposure to the inflammatory stimulus TNFα, TAV endothelial colony forming cells (ECFCs) upregulate the expression of phosphate transporter 2 (PiT2), whereas BAV ECFCs did not increase the expression of PiT2 at all [32]. Therefore, it would be of future interest to study how an increase in the NFκB signaling pathway, will affect the aortic EC response and the underlying vascular remodeling in BAV patients.

Research has shown that oscillatory flow can cause an increase of SNAI1 in endothelial cells [33]. Consistent with this, our data indicates a trend towards increased expression of SNAI1 in endothelial cells at the non-jet side of BAV aortas, indicating an activated phenotype. Interestingly, we observed SNAI1 expression in adventitial vessels in both the jet and non-jet samples. This observation suggests ongoing EndoMT in the adventitia, but requires further evaluation. In addition, a trend towards higher KI67$^+$ ECs at the BAV non-jet side could be observed. However, although proliferation is associated with an activated EC phenotype *in vitro*, it is unclear what a normal proliferative rate is *in vivo* and therefore requires further research [34].

Vasoprotective transcription factors KLF2 and KLF4 have been reported to be upregulated by laminar shear stress [35,36]. Since the analysis in this study focussed on the location with the most severe morphology, the lack of KLF2 and KLF4 in the endothelium studied can be a result of a life long exposure to these flow conditions and/or advanced pathogenesis. This hypothesis is supported by the presence of endothelial expression of KLF2 and KLF4 at distant locations, where the vascular remodeling was less severe.

These results together support the hypothesis that in BAV patients the ECs at the non-jet side of the aorta have an activated phenotype. However, since vWF$^+$ area is higher in the jet side and EC proliferation, inflammation and EndoMT are higher at the non-jet side, further research should be performed to relate activation of ECs to expression vWF expression.

Methods

Patient material

For this study, sample collection and handling were carried out according to the official guidelines of the Medical Ethical Committee of the Central Hospital Bad Berka [12]. All patients gave written informed consent. Aortic samples from BAV (n=23) patients were collected during aortic and aortic valve replacement surgery with or without concomitant proximal aortic replacement. Jet-side and non-jet side of the ascending aorta were determined based on preoperative MRI analysis. A valve was considered a BAV if only two commissures were present. Patients with genetic disorders (e.g. Marfan syndrome) were excluded. Aortic valve stenosis and regurgitation were defined according to the valvular guidelines [37]. The diameter of the proximal aorta was measured preoperatively by means of transthoracic echocardiography and MRI. Dilation was defined by reaching an ascending aortic wall diameter of 45 mm or more [38]. Samples were fixed in 4% formalin (24 hours) and decalcified in a formic acid-formate buffer (120 hours) prior to embedding in paraffin. Transverse sections (5 μm) were mounted on Starfrost slides (Klinipath, Radnor, PA, USA).

Elastin visualization

Sections were deparaffinised, rehydrated and incubated with Weigert's resorcin fuchsin (RF, Klinipath) according to the manufacturer's protocol to study the elastin morphology of the vessel wall.

Immunohistochemistry

To stain for vWF, a staining based on DAB was used. To this end, sections were deparaffinised, rehydrated and endogenous peroxidase activity was inhibited by exposure to 0.3% H_2O_2 for 20 min before antigen retrieval by heating the sections to 97°C in sodium citrate buffer (pH 6.0) for 11 minutes. Subsequently, sections were incubated o/n at rt with the primary antibodies diluted in PBS-Tween-20 (PBST) containing 1% bovine serum albumin (BSA, A8022; Sigma-Aldrich, St Louis, MO, USA, 1%BSA-PBST, polyclonal rabbit anti-vWF antibody (A 0082). A list of all primary antibodies can be found in Supplemental Table 1. The following day, the sections were incubated with a biotin-conjugated secondary antibody in PBST containing 1,5% normal goat serum for 60 minutes, followed by a 75 minute incubation with the ABC-cocktail (1:100 compound A and 1:100 compound B, Vector Laboratories, Burlingame, Calif; PK610) after a pre-incubation of the cocktail of at least 45 minutes. For visualization, slides were incubated with 400mg/ml 3,30-diaminobenzidine tetrachloride (Sigma-Aldrich Chemie,

Buchs, Switzerland; D5637) dissolved in Tris-maleate buffer with 20 ml of H2O2 for 5 minutes. Counterstaining was performed using 0,1% haematoxylin (Merck, Darmstadt, Germany) for 5 seconds. After dehydration, the sections were mounted using Entellan (Merck).

For the immunofluorescent stainings, sections were deparaffinised, rehydrated and antigen retrieval was performed as described above. Sections were incubated o/n at room temperature with the primary antibodies diluted in 1%BSA-PBST before incubating the with the secondary antibodies diluted in 1%BSA-PBST for 40 minutes and 4',6-Diamidine-2'-phenylindole dihydrochloride (DAPI, D3571 Life Technologies 1:1000) for 5 minutes to stain for nuclei. Sections were mounted using Prolong Gold (Invitrogen, Carlsbad, CA, USA; P36934) Between the staining steps, all sections were rinsed in PBS (2x) and PBST (1x). All sections used for quantitative analysis were stained at the same time.

Sample selection for double positive analysis

Sections from all of the patients were stained for PECAM and α-SMA and scanned with Panoramic 250 Slidescanner (3DHISTECH Ltd.) at 40x magnification. Additionally, only the patient samples containing continuous a endothelial layer on both the jet side and non-jet side were selected for further examination.

Quantification of images

No images were taken from areas with ruptured intimal tissue. To quantify the vWF^+ positive area the surface area positive for vWF the stained sections were scanned with a Panoramic 250 Slidescanner. A representative number of images of the intima and media (up to 500 μm from the intimal edge) were taken randomly divided over the section. The number of images varied based on the size of the tissue but was at least 2 per sample. The area of vWF was calculated by determining threshold appropriate to each individual image in a blinded manner using ImageJ2. The percentage of vWF^+ area per image was calculated. An average of all images per tissue as well as the images with the lowest and highest percentages were used in the analysis.

To quantify the thickness of the intima, the inner elastic lamellae up to the lumen was measured every 100 μm. There were at least 2 measurements per sample. EC positive for PECAM and ECs double positive for PECAM and either p50, SNAI1 or ki67 were quantified. To standardize the area in which the ECs were quantified, the location with the least structured SMC and elastic lamellar organization in the inner media was selected. All subsequent analysis was focused on endothelium in the selected location. Images were made using a Leica DM500 microscope and the 40x magnification lens. The positive ECs in

the images were manually counted twice by two different, blinded observers. Discrepancies in the observations were studied until a consensus was achieved.

Statistical analysis

A paired sample t-test was performed to assess the flow induced differences between the two aortic wall sides. Statistical analysis was performed using the GraphPad Prism 7 (GraphPad Software, Inc.), applying a significance level of $p < 0.05$. Graphs are depicted with standard error of the mean (SEM).

Acknowledgements

We gratefully thank dr. R. Fontijn for providing the KLF2 antibody.

Funding

This work is supported by the Dutch Heart Foundation (BAV consortium grant 31190).

Supplementals

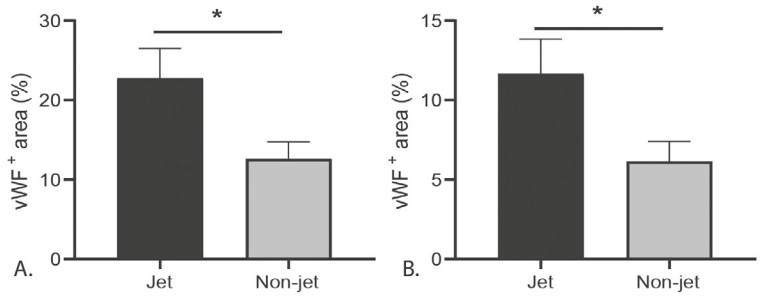

Supplemental figure 1. Quantification of intimal and inner media vWF+area on jet and non-jet side of BAV patient aortas. A,B. Quantification using the highest measurement of vWF+ area per sample (A) or the lowest measurement of vWF+ area per sample (B) as % of the surface area of the inner media (500 μm). *p>0.05.

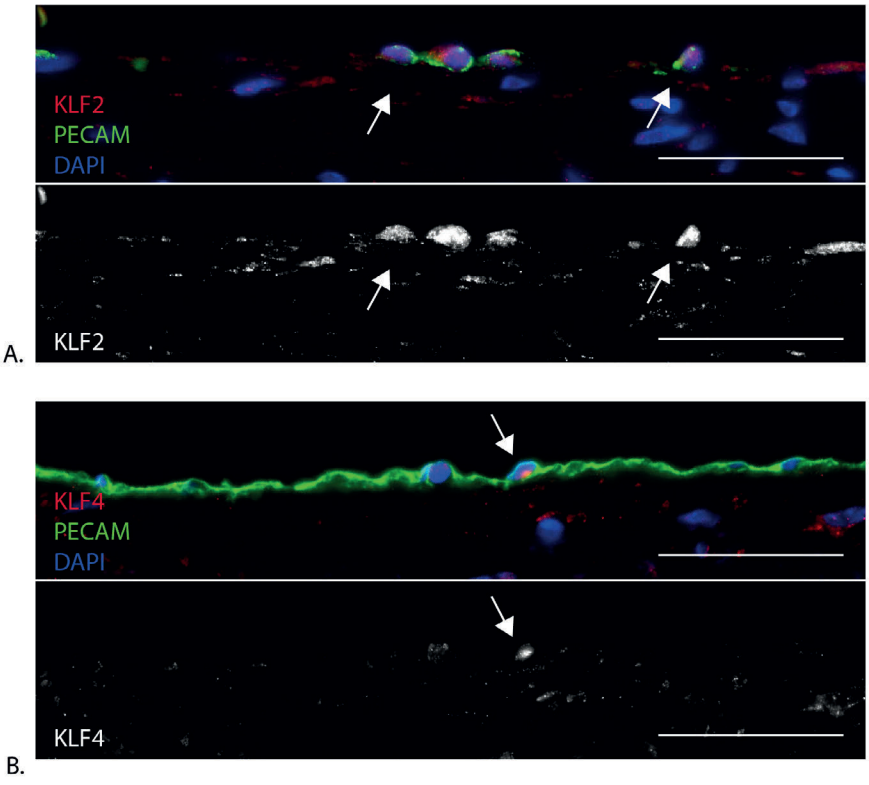

Supplemental figure 2. Pictures of KLF2/4 staining. A. KLF2 positive ECs in a remote area. B. KLF4 positive ECs in a remote area. Bar indicates 50 μm. Arrows indicate KLF2/4 -PECAM positive cells.

Supplemental table 1. List of primary antibodies

Target	Host	Supplier	Reference	Concentration
PECAM-1	Rabbit	Santa Cruz	SC-1506-R	1:500
PECAM-1	Goat	R&D Systems	AF3628	1:1000
SNAI1	Goat	R&D Systems	AF3639	1:100
NFκB p50	Mouse	Santa Cruz	SC-7386	1:200
α-SMA	Mouse	Sigma-Aldrich	A2547	1:10.000
KI-67	Rabbit	ABcam	AB15580	1:300
KLF2	Rabbit	Manufactured at VUmc	*	1:200
KLF4	Rabbit	ABcam	AB34814	1:200

References

1. Ward, C. (2000). Clinical significance of the bicuspid aortic valve. *Heart*
2. Wang, X, et al. (2005). Decreased expression of fibulin-5 correlates with reduced elastin in thoracic aortic dissection. *Surgery*
3. Tsamis, A, et al. (2013). Elastin and collagen fibre microstructure of the human aorta in ageing and disease: A review. *Journal of the Royal Society, Interface*
4. Cohen, JR, et al. (1992). Smooth muscle cell elastase, atherosclerosis, and abdominal aortic aneurysms. *Ann Surg*
5. Nathan, CF. (1987). Secretory products of macrophages. *J Clin Invest*
6. Barker, AJ, et al. (2010). Quantification of hemodynamic wall shear stress in patients with bicuspid aortic valve using phase-contrast mri. *Annals of biomedical engineering*
7. Barker, AJ, et al. (2012). Bicuspid aortic valve is associated with altered wall shear stress in the ascending aorta. *Circ Cardiovasc Imaging*
8. Cotrufo, M, et al. (2005). Different patterns of extracellular matrix protein expression in the convexity and the concavity of the dilated aorta with bicuspid aortic valve: Preliminary results. *J Thorac Cardiovasc Surg*
9. Bissell, MM, et al. (2013). Aortic dilation in bicuspid aortic valve disease: Flow pattern is a major contributor and differs with valve fusion type. *Circ Cardiovasc Imaging*
10. Mahadevia, R, et al. (2014). Bicuspid aortic cusp fusion morphology alters aortic three-dimensional outflow patterns, wall shear stress, and expression of aortopathy. *Circulation*
11. Atkins, SK, et al. (2014). Etiology of bicuspid aortic valve disease: Focus on hemodynamics. *World J Cardiol*
12. Grewal, N, et al. (2017). The effects of hemodynamics on the inner layers of the aortic wall in patients with a bicuspid aortic valve. *Integr Mol Med*
13. Chatzizisis, YS, et al. (2007). Role of endothelial shear stress in the natural history of coronary atherosclerosis and vascular remodeling: Molecular, cellular, and vascular behavior. *J Am Coll Cardiol*
14. Wang, C, et al. (2013). Endothelial cell sensing of flow direction. *Arterioscler Thromb Vasc Biol*
15. Wagner, DD, et al. (2008). The vessel wall and its interactions. *Blood*
16. Sievers, HH, et al. (2014). Toward individualized management of the ascending aorta in bicuspid aortic valve surgery: The role of valve phenotype in 1362 patients. *J Thorac Cardiovasc Surg*
17. Kong, WKF, et al. (2020). Sex differences in bicuspid aortic valve disease. *Progr Cardiovasc Dis*
18. Nayak, L, et al. (2011). "Go with the flow": How krüppel-like factor 2 regulates the vasoprotective effects of shear stress. *Antioxid Redox Signal*

19. Brott, DA, et al. (2014). Evaluation of von willebrand factor and von willebrand factor propeptide in models of vascular endothelial cell activation, perturbation, and/or injury. *Toxicol Pathol*
20. Lenting, PJ, et al. (2015). Von willebrand factor biosynthesis, secretion, and clearance: Connecting the far ends. *Blood*
21. Gogia, S, et al. (2015). Role of fluid shear stress in regulating vwf structure, function and related blood disorders. *Biorheology*
22. Ling, J, et al. (2019). Feedback modulation of endothelial cells promotes epithelial-mesenchymal transition and metastasis of osteosarcoma cells by von willebrand factor release. *J Cell Biochem*
23. Grewal, N, et al. (2019). The role of hemodynamics in bicuspid aortopathy: A histopathologic study. *Cardiovasc Pathol*
24. Guzzardi, DG, et al. (2015). Valve-related hemodynamics mediate human bicuspid aortopathy: Insights from wall shear stress mapping. *J Am Coll Cardiol*
25. Peters, DG, et al. (2002). Genomic analysis of immediate/early response to shear stress in human coronary artery endothelial cells. *Physiol Genomics*
26. Takahashi, M, et al. (1997). Mechanotransduction in endothelial cells: Temporal signaling events in response to shear stress. *J Vasc Res*
27. Chatzizisis, YS, et al. (2007). Role of endothelial shear stress in the natural history of coronary atherosclerosis and vascular remodeling: Molecular, cellular, and vascular behavior. *Journal of the American College of Cardiology*
28. Zamboni, P, et al. (2016). Oscillatory flow suppression improves inflammation in chronic venous disease. *J Surg Res*
29. Wang, F, et al. (2019). Oscillating flow promotes inflammation through the tlr2-tak1-ikk2 signalling pathway in human umbilical vein endothelial cell (huvecs). *Life Sci*
30. Tobin, SW, et al. (2019). Novel mediators of aneurysm progression in bicuspid aortic valve disease. *J Mol Cell Cardiol*
31. Grewal, N, et al. (2016). Histopathology of aortic complications in bicuspid aortic valve versus marfan syndrome: Relevance for therapy? *Heart and vessels*
32. van de Pol, V, et al. (2019). Endothelial colony forming cells as an autologous model to study endothelial dysfunction in patients with a bicuspid aortic valve. *Int J Mol Sci*
33. Bjorck, HM, et al. (2018). Altered DNA methylation indicates an oscillatory flow mediated epithelial-to-mesenchymal transition signature in ascending aorta of patients with bicuspid aortic valve. *Sci Rep*
34. Li, Y-SJ, et al. (2005). Molecular basis of the effects of shear stress on vascular endothelial cells. *Journal of Biomechanics*
35. Dekker, RJ, et al. (2006). Klf2 provokes a gene expression pattern that establishes functional quiescent differentiation of the endothelium. *Blood*

36. Villarreal, G, Jr., et al. (2010). Defining the regulation of klf4 expression and its downstream transcriptional targets in vascular endothelial cells. *Biochem Biophys Res Commun*
37. Baumgartner, H, et al. (2009). Echocardiographic assessment of valve stenosis: Eae/ase recommendations for clinical practice. *J Am Soc Echocardiogr*
38. Hiratzka, LF, et al. (2016). Surgery for aortic dilatation in patients with bicuspid aortic valves: A statement of clarification from the american college of cardiology/american heart association task force on clinical practice guidelines. *J Am Coll Cardiol*